Acta Crystallographica Section B
Structural Science
ISSN 0108-7681

Torsional vibration and central bond length of *N*-benzylideneanilines

Jun Harada, Mayuko Harakawa and Keiichiro Ogawa*

Department of Chemistry, Graduate School of Arts and Sciences, The University of Tokyo, Komaba, Meguro-ku, Tokyo 153-8902, Japan

Correspondence e-mail: ogawa@ramie.c.u-tokyo.ac.jp

Received 12 March 2004
Accepted 7 July 2004

The crystal structures of *N*-benzylideneaniline (1), *N*-benzylidene-4-carboxyaniline (2), *N*-(4-methylbenzylidene)-4-nitroaniline (3), *N*-(4-nitrobenzylidene)-4-methoxyaniline (4), *N*-(4-nitrobenzylidene)-4-methylaniline (5), *N*-(4-methoxybenzylidene)aniline (6) and *N*-(4-methoxybenzylidene)-4-methylaniline (7) were determined by X-ray diffraction analyses at various temperatures. In the crystal structures of all the compounds, an apparent shortening of the central C=N bond was observed at room temperature. As the temperature was lowered, the observed bond lengths increased to approximately 1.28 Å at 90 K, irrespective of substituents in the molecules. The shortening and the temperature dependence of the C=N bond length are interpreted in terms of an artifact caused by the torsional vibration of the C—Ph and N—Ph bonds in the crystals. In the crystal structures of (1) and (7), a static disorder around the C=N bond was observed, which is also responsible for the apparent shortening of the C=N bond.

1. Introduction

The molecular structure of *N*-benzylideneaniline has attracted considerable attention and has been studied extensively for over half a century. At an early stage of the studies, there were many arguments about the origin of the marked difference in the UV spectrum of *N*-benzylideneaniline from its isoelectronic molecules, (*E*)-stilbene and azobenzene (Wiegand & Merkel, 1942; Izmailskii & Smirnov, 1956; Jaffe *et al.*, 1958; Ebara, 1960). About 35 years ago, Bürgi and Dunitz carried out X-ray diffraction analyses of *N*-benzylideneaniline (1), *N*-benzylidene-4-carboxyaniline (2) and *N*-(4-methylbenzylidene)-4-nitroaniline (3), and revealed that the aniline ring of the *N*-benzylideneanilines is twisted out of the C—N=C—C plane by 40–55°, in sharp contrast to (*E*)-stilbene and azobenzene which have almost planar structures in the crystals (Bürgi & Dunitz, 1969, 1970). The difference in the planarity of the molecules has then been the most cogent explanation for the difference in the UV spectra.

In spite of its success in solving the problem of the UV spectrum, the crystallographic study produced a new problem in the structure of *N*-benzylideneanilines, as the length of the central C=N bond was reported to vary with the compound [(1) 1.237 (3), (2) 1.281 (12) and (3) 1.269 (5) Å]. In their study the crystal structures were determined using an early four-circle diffractometer and the true uncertainties in the bond lengths were expected to be larger than the estimated standard deviations given in the parentheses (Bürgi & Dunitz, 1970). The remarkable shortening of the C=N bond lengths of (1), however, should be regarded as significant and having some latent cause. The length of the N—Ph bond was also

Table 1
Experimental details.

RT = room temperature.

	(1) RT	(1) 90 K	(2) RT	(2) 90 K	(3) RT
Crystal data					
Chemical formula	$C_{13}H_{11}N$	$C_{13}H_{11}N$	$C_{14}H_{11}NO_2$	$C_{14}H_{11}NO_2$	$C_{14}H_{12}N_2O_2$
M_r	181.23	181.23	225.24	225.24	240.26
Cell setting, space group	Monoclinic, $P2_1/c$	Monoclinic, $P2_1/c$	Monoclinic, $P2_1/c$	Monoclinic, $P2_1/c$	Monoclinic, $P2_1/c$
a, b, c (Å)	11.9503 (19), 7.9347 (13), 12.1664 (19)	11.8429 (9), 7.7182 (5), 12.1211 (9)	6.6639 (7), 30.878 (3), 7.6091 (9)	6.6193 (5), 30.381 (2), 7.5764 (6)	15.5033 (12), 7.2979 (5), 12.7983 (8)
β (°)	118.321 (3)	118.341 (1)	133.576 (2)	134.151 (1)	123.625 (1)
V (Å^3)	1015.6 (3)	975.14 (12)	1134.3 (2)	1093.21 (14)	1205.74 (15)
Z	4	4	4	4	4
D_x (Mg m^{-3})	1.185	1.234	1.319	1.369	1.324
Radiation type	Mo $K\alpha$	Mo $K\alpha$	Mo $K\alpha$	Mo $K\alpha$	Mo $K\alpha$
No. of reflections for cell parameters	2949	6138	8458	11 149	4693
θ range (°)	3.2–23.8	3.3–30.0	2.6–30.0	3.2–30.0	2.8–27.3
μ (mm^{-1})	0.07	0.07	0.09	0.09	0.09
Temperature (K)	300	90	300	90	300
Crystal form, colour	Block, colourless	Block, colourless	Block, pale yellow	Block, pale yellow	Plate, pale yellow
Crystal size (mm)	0.36 × 0.30 × 0.01	0.36 × 0.30 × 0.01	0.70 × 0.66 × 0.16	0.70 × 0.66 × 0.16	0.60 × 0.56 × 0.04
Data collection					
Diffractometer	Bruker SMART 1000CCD	Bruker SMART 1000CCD	Bruker SMART 1000CCD	Bruker SMART 1000CCD	Bruker SMART 1000CCD
Data collection method	ω scan	ω scan	ω scan	ω scan	ω scan
Absorption correction	Multi-scan (based on symmetry-related measurements)	Multi-scan (based on symmetry-related measurements)	Multi-scan (based on symmetry-related measurements)	Multi-scan (based on symmetry-related measurements)	Multi-scan (based on symmetry-related measurements)
T_{min}	0.976	0.975	0.940	0.938	0.948
T_{max}	0.999	0.999	0.986	0.985	0.996
No. of measured, independent and observed reflections	15 417, 2966, 1781	14 636, 2834, 2406	17 030, 3305, 2783	16 650, 3193, 3046	16 372, 3506, 2359
Criterion for observed reflections	$I > 2\sigma(I)$	$I > 2\sigma(I)$	$I > 2\sigma(I)$	$I > 2\sigma(I)$	$I > 2\sigma(I)$
R_{int}	0.023	0.019	0.024	0.018	0.023
θ_{max} (°)	30.1	30.0	30.0	30.0	30.0
Range of h, k, l	$-16 \Rightarrow h \Rightarrow 16$ $-11 \Rightarrow k \Rightarrow 11$ $-17 \Rightarrow l \Rightarrow 17$	$-16 \Rightarrow h \Rightarrow 16$ $-10 \Rightarrow k \Rightarrow 10$ $-17 \Rightarrow l \Rightarrow 16$	$-9 \Rightarrow h \Rightarrow 9$ $-43 \Rightarrow k \Rightarrow 43$ $-10 \Rightarrow l \Rightarrow 10$	$-9 \Rightarrow h \Rightarrow 9$ $-42 \Rightarrow k \Rightarrow 42$ $-10 \Rightarrow l \Rightarrow 10$	$-21 \Rightarrow h \Rightarrow 21$ $-10 \Rightarrow k \Rightarrow 10$ $-18 \Rightarrow l \Rightarrow 18$
Refinement					
Refinement on	F^2	F^2	F^2	F^2	F^2
$R[F^2 > 2\sigma(F^2)]$, $wR(F^2)$, S	0.046, 0.135, 1.00	0.035, 0.103, 1.04	0.060, 0.160, 1.11	0.045, 0.113, 1.13	0.044, 0.125, 1.02
No. of reflections	2966	2834	3305	3193	3506
No. of parameters	175	159	202	202	219
H-atom treatment	Mixture of independent and constrained refinement	Constrained to parent site	Mixture of independent and constrained refinement	Mixture of independent and constrained refinement	Mixture of independent and constrained refinement
Weighting scheme	$w = 1/[\sigma^2(F_o^2) + (0.0552P)^2 + 0.1448P]$, where $P = (F_o^2 + 2F_c^2)/3$	$w = 1/[\sigma^2(F_o^2) + (0.0577P)^2 + 0.1821P]$, where $P = (F_o^2 + 2F_c^2)/3$	$w = 1/[\sigma^2(F_o^2) + (0.0516P)^2 + 0.6951P]$, where $P = (F_o^2 + 2F_c^2)/3$	$w = 1/[\sigma^2(F_o^2) + (0.0447P)^2 + 0.6769P]$, where $P = (F_o^2 + 2F_c^2)/3$	$w = 1/[\sigma^2(F_o^2) + (0.0475P)^2 + 0.2849P]$, where $P = (F_o^2 + 2F_c^2)/3$
$(\Delta/\sigma)_{max}$	<0.0001	<0.0001	<0.0001	<0.0001	<0.0001
$\Delta\rho_{max}$, $\Delta\rho_{min}$ (e Å^{-3})	0.18, −0.16	0.36, −0.19	0.23, −0.22	0.48, −0.21	0.20, −0.16
Extinction method	None	None	None	None	None

	(3) 90 K	(4) RT	(4) 90 K	(5) RT	(5) 90 K
Crystal data					
Chemical formula	$C_{14}H_{12}N_2O_2$	$C_{14}H_{12}N_2O_3$	$C_{14}H_{12}N_2O_3$	$C_{14}H_{12}N_2O_2$	$C_{14}H_{12}N_2O_2$
M_r	240.26	256.26	256.26	240.26	240.26
Cell setting, space group	Monoclinic, $P2_1/c$	Monoclinic, $P2_1/c$	Monoclinic, $P2_1/c$	Triclinic, $P\bar{1}$	Triclinic, $P\bar{1}$
a, b, c (Å)	15.4449 (13), 7.1070 (5), 12.6557 (9)	12.8889 (8), 7.1007 (4), 14.0304 (8)	12.7478 (7), 6.9429 (4), 13.9980 (8)	7.1098 (5), 12.5649 (9), 14.3814 (10)	6.9610 (4), 12.3496 (7), 14.3296 (8)
α, β, γ (°)	90.00, 123.370 (1), 90.00	90.00, 102.815 (1), 90.00	90.00, 102.446 (1), 90.00	72.617 (1), 83.926 (1), 86.144 (1)	73.168 (1), 82.719 (1), 85.061 (1)
V (Å^3)	1160.15 (15)	1252.08 (13)	1209.80 (12)	1218.33 (15)	1167.99 (11)

Table 1 (continued)

	(3) 90 K	(4) RT	(4) 90 K	(5) RT	(5) 90 K
Z	4	4	4	4	4
D_x (Mg m^{-3})	1.376	1.359	1.407	1.310	1.366
Radiation type	Mo $K\alpha$	Mo $K\alpha$	Mo $K\alpha$	Mo $K\alpha$	Mo $K\alpha$
No. of reflections for cell parameters	6799	5863	10 589	5945	11 270
θ range (°)	3.2–30.0	2.9–29.3	2.9–30.0	2.6–29.8	3.0–30.0
μ (mm^{-1})	0.09	0.10	0.10	0.09	0.09
Temperature (K)	90	300	90	300	90
Crystal form, colour	Plate, pale yellow	Prism, yellow	Prism, yellow	Block, yellow	Block, yellow
Crystal size (mm)	0.60 × 0.56 × 0.04	0.58 × 0.48 × 0.18	0.58 × 0.48 × 0.18	0.50 × 0.36 × 0.18	0.50 × 0.36 × 0.18
Data collection					
Diffractometer	Bruker SMART 1000CCD	Bruker SMART 1000CCD	Bruker SMART 1000CCD	Bruker SMART 1000CCD	Bruker SMART 1000CCD
Data collection method	ω scan	ω scan	ω scan	ω scan	ω scan
Absorption correction	Multi-scan (based on symmetry-related measurements)	Multi-scan (based on symmetry-related measurements)	Multi-scan (based on symmetry-related measurements)	Multi-scan (based on symmetry-related measurements)	Multi-scan (based on symmetry-related measurements)
T_{min}	0.946	0.946	0.944	0.957	0.955
T_{max}	0.996	0.983	0.982	0.984	0.983
No. of measured, independent and observed reflections	15 616, 3365, 2780	18 959, 3649, 2515	18 152, 3530, 3163	18 799, 7068, 4658	18 035, 6782, 6118
Criterion for observed reflections	$I > 2\sigma(I)$	$I > 2\sigma(I)$	$I > 2\sigma(I)$	$I > 2\sigma(I)$	$I > 2\sigma(I)$
R_{int}	0.019	0.022	0.017	0.026	0.014
θ_{max} (°)	30.0	30.0	30.0	30.0	30.0
Range of h, k, l	$-21 \Rightarrow h \Rightarrow 21$ $-9 \Rightarrow k \Rightarrow 9$ $-17 \Rightarrow l \Rightarrow 17$	$-18 \Rightarrow h \Rightarrow 18$ $-9 \Rightarrow k \Rightarrow 9$ $-19 \Rightarrow l \Rightarrow 19$	$-17 \Rightarrow h \Rightarrow 17$ $-9 \Rightarrow k \Rightarrow 9$ $-19 \Rightarrow l \Rightarrow 19$	$-10 \Rightarrow h \Rightarrow 9$ $-17 \Rightarrow k \Rightarrow 17$ $-20 \Rightarrow l \Rightarrow 20$	$-9 \Rightarrow h \Rightarrow 9$ $-17 \Rightarrow k \Rightarrow 17$ $-20 \Rightarrow l \Rightarrow 20$
Refinement					
Refinement on	F^2	F^2	F^2	F^2	F^2
$R[F^2 > 2\sigma(F^2)]$, $wR(F^2)$, S	0.037, 0.110, 1.05	0.046, 0.141, 1.02	0.038, 0.111, 1.05	0.050, 0.150, 1.04	0.038, 0.111, 1.03
No. of reflections	3365	3649	3530	7068	6782
No. of parameters	219	220	220	438	438
H-atom treatment	Mixture of independent and constrained refinement	Refined independently	Refined independently	Mixture of independent and constrained refinement	Mixture of independent and constrained refinement
Weighting scheme	$w = 1/[\sigma^2(F_o^2) + (0.0626P)^2 + 0.3251P]$, where $P = (F_o^2 + 2F_c^2)/3$	$w = 1/[\sigma^2(F_o^2) + (0.0613P)^2 + 0.2307P]$, where $P = (F_o^2 + 2F_c^2)/3$	$w = 1/[\sigma^2(F_o^2) + (0.0659P)^2 + 0.2901P]$, where $P = (F_o^2 + 2F_c^2)/3$	$w = 1/[\sigma^2(F_o^2) + (0.0637P)^2 + 0.1715P]$, where $P = (F_o^2 + 2F_c^2)/3$	$w = 1/[\sigma^2(F_o^2) + (0.0698P)^2 + 0.2469P]$, where $P = (F_o^2 + 2F_c^2)/3$
$(\Delta/\sigma)_{max}$	0.001	<0.0001	0.001	0.001	0.001
$\Delta\rho_{max}$, $\Delta\rho_{min}$ (e Å^{-3})	0.45, −0.16	0.16, −0.23	0.40, −0.26	0.19, −0.25	0.44, −0.31
Extinction method	None	None	None	*SHELXL*	*SHELXL*
Extinction coefficient	–	–	–	0.029 (3)	0.021 (2)

	(6) RT	(6) 90 K	(7) RT	(7) 90 K
Crystal data				
Chemical formula	$C_{14}H_{13}NO$	$C_{14}H_{13}NO$	$C_{15}H_{15}NO$	$C_{15}H_{15}NO$
M_r	211.25	211.25	225.28	225.28
Cell setting, space group	Monoclinic, $P2_1/n$	Monoclinic, $P2_1/n$	Orthorhombic, $Pna2_1$	Orthorhombic, $Pna2_1$
a, b, c (Å)	10.2529 (6), 12.6440 (7), 18.2037 (10)	10.0666 (13), 12.6374 (17), 17.732 (2)	12.2403 (8), 13.8088 (9), 7.4287 (5)	12.0319 (17), 13.8190 (19), 7.263 (1)
β (°)	95.998 (1)	95.226 (3)	90.00	90.00
V (Å^3)	2347.0 (2)	2246.4 (5)	1255.63 (14)	1207.6 (3)
Z	8	8	4	4
D_x (Mg m^{-3})	1.196	1.249	1.192	1.239
Radiation type	Mo $K\alpha$	Mo $K\alpha$	Mo $K\alpha$	Mo $K\alpha$
No. of reflections for cell parameters	7226	11 566	5061	7926
θ range (°)	2.2–25.3	2.3–30.0	2.2–26.8	2.2–30.0
μ (mm^{-1})	0.08	0.08	0.08	0.08
Temperature (K)	300	90	300	90
Crystal form, colour	Block, colourless	Block, colourless	Rod, pale yellow	Rod, pale yellow
Crystal size (mm)	0.46 × 0.40 × 0.20	0.46 × 0.40 × 0.20	0.62 × 0.22 × 0.20	0.62 × 0.22 × 0.20

Table 1 (continued)

	(6) RT	(6) 90 K	(7) RT	(7) 90 K
Data collection				
Diffractometer	Bruker SMART 1000CCD	Bruker SMART 1000CCD	Bruker SMART 1000CCD	Bruker SMART 1000CCD
Data collection method	ω scan	ω scan	ω scan	ω scan
Absorption correction	Multi-scan (based on symmetry-related measurements)	Multi-scan (based on symmetry-related measurements)	Multi-scan (based on symmetry-related measurements)	Multi-scan (based on symmetry-related measurements)
T_{min}	0.966	0.965	0.955	0.954
T_{max}	0.985	0.984	0.985	0.985
No. of measured, independent and observed reflections	35 497, 6867, 3566	33 475, 6556, 5379	18 683, 3664, 2677	17 826, 3523, 3375
Criterion for observed reflections	$I > 2\sigma(I)$	$I > 2\sigma(I)$	$I > 2\sigma(I)$	$I > 2\sigma(I)$
R_{int}	0.039	0.027	0.023	0.020
θ_{max} (°)	30.1	30.0	30.0	30.0
Range of h, k, l	$-14 \Rightarrow h \Rightarrow 14$ $-17 \Rightarrow k \Rightarrow 17$ $-25 \Rightarrow l \Rightarrow 25$	$-14 \Rightarrow h \Rightarrow 14$ $-17 \Rightarrow k \Rightarrow 17$ $-24 \Rightarrow l \Rightarrow 24$	$-17 \Rightarrow h \Rightarrow 17$ $-19 \Rightarrow k \Rightarrow 19$ $-10 \Rightarrow l \Rightarrow 10$	$-16 \Rightarrow h \Rightarrow 16$ $-19 \Rightarrow k \Rightarrow 19$ $-10 \Rightarrow l \Rightarrow 10$
Refinement				
Refinement on	F^2	F^2	F^2	F^2
$R[F^2 > 2\sigma(F^2)]$, $wR(F^2)$, S	0.057, 0.147, 1.01	0.043, 0.118, 1.03	0.055, 0.161, 1.05	0.034, 0.093, 1.03
No. of reflections	6867	6556	3664	3523
No. of parameters	393	393	203	186
H-atom treatment	Refined independently	Refined independently	Mixture of independent and constrained refinement	Constrained to parent site
Weighting scheme	$w = 1/[\sigma^2(F_o^2) + (0.0208P)^2 + 0.8084P]$, where $P = (F_o^2 + 2F_c^2)/3$	$w = 1/[\sigma^2(F_o^2) + (0.0608P)^2 + 0.6548P]$, where $P = (F_o^2 + 2F_c^2)/3$	$w = 1/[\sigma^2(F_o^2) + (0.0814P)^2 + 0.1711P]$, where $P = (F_o^2 + 2F_c^2)/3$	$w = 1/[\sigma^2(F_o^2) + (0.0587P)^2 + 0.1458P]$, where $P = (F_o^2 + 2F_c^2)/3$
$(\Delta/\sigma)_{max}$	<0.0001	0.001	<0.0001	<0.0001
$\Delta\rho_{max}$, $\Delta\rho_{min}$ (e Å^{-3})	0.16, −0.20	0.35, −0.25	0.26, −0.17	0.33, −0.15
Extinction method	None	None	None	None
Absolute structure	–	–	Flack (1983)	Flack (1983)
Flack parameter	–	–	−2 (2)	−0.8 (10)

Computer programs used: *SMART* and *SAINT* (Bruker, 1998), *SHELXS*97 (Sheldrick, 1990), *SHELXL*97 (Sheldrick, 1997), *SHELXTL* (Bruker, 2000).

reported to vary with the compound [(1) 1.460 (3) Å, (2) 1.431 (7) Å and (3) 1.400 (3) Å]. Since the reported structures have been used as the standard experimental molecular structures of *N*-benzylideneanilines, the availability of accurate molecular structures of the compounds has considerable significance.

The shortening or anomaly in the central bonds of *N*-benzylideneanilines has reminded us of our recent studies on the ethylene bond length of (*E*)-stilbenes, which have a molecular skeleton similar to *N*-benzylideneanilines (Ogawa *et al.*, 1992, 1995). For the crystal structures of (*E*)-stilbenes, it was shown that the central C═C bond length measured at room temperature was anomalously short. As the temperature was lowered, the bond length increased significantly. The shortening of the observed bond length and its temperature dependence were shown to be artifacts caused by the torsional vibration of the C—Ph bonds in the crystals. A similar phenomenon, *i.e.* an apparent shortening of the central bond at room temperature, was observed in the crystal structures of azobenzenes and 1,2-diphenylethanes (Harada *et al.*, 1995, 1997; Harada & Ogawa, 2001). It was therefore expected that the anomalous bond lengths of *N*-benzylideneanilines are also artifacts caused by the torsional vibration of the C—Ph and N—Ph bonds.

To examine the above hypothesis, we carried out variable-temperature X-ray crystallographic analyses of (1) and its derivatives, (2), (3), *N*-(4-nitrobenzylidene)-4-methoxyaniline (4), *N*-(4-nitrobenzylidene)-4-methylaniline (5), *N*-(4-methoxybenzylidene)aniline (6) and *N*-(4-methoxybenzylidene)-4-methylaniline (7).

2. Experimental

All compounds were obtained by the dehydration condensation between the corresponding benzaldehyde and aniline. Crystals of (1), (4) and (7) were obtained by recrystallization from methanol. Crystals of (2), (3), (5) and (6) were obtained from diethylether, 2-propanol, ethanol and hexane, respectively. Melting points were determined on a micro-hot-stage apparatus and are uncorrected.

All diffraction measurements were carried out using a Bruker SMART 1000CCD area-detector system with graphite-monochromated Mo $K\alpha$ radiation (λ = 0.71073 Å). About 2500 frames of data were collected for each data set with a scan width of 0.3° in ω and 5, 10 or 20 s exposure times. A semi-empirical absorption correction was applied to the data using the *SADABS* program (Sheldrick, 2002). The measurements at 90 K were carried out using a Cryostream

(Oxford Cryosystems) open-flow gas cryostat (Cosier & Glazer, 1986). The temperature in the nozzle was held constant within ± 0.2 K during the measurement. For the measurements of (1), a crystal was enclosed in a Lindemann-glass capillary to prevent sublimation. For non-disordered molecules, all H atoms were located from difference-Fourier electron density maps and refined isotropically, and all C, N and O atoms were refined anisotropically. For disordered molecules, the refinement procedures are given in *Appendix A*. The crystal and experimental data are summarized in Table 1.[1]

Molecular orbital calculations were performed using the *GAUSSIAN* 98 program (Frisch *et al.*, 1998). Geometry optimization was carried out at the MP2/6-31G* or B3LYP/6-31G* level.

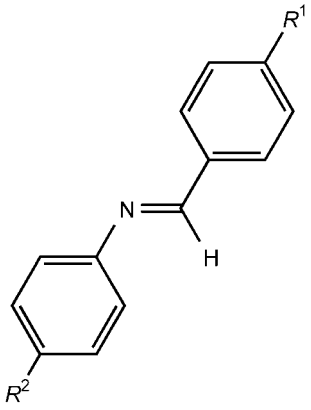

	R^1	R^2
(1)	H	H
(2)	H	COOH
(3)	CH_3	NO_2
(4)	NO_2	OCH_3
(5)	NO_2	CH_3
(6)	OCH_3	H
(7)	OCH_3	CH_3

3. Results and discussion

Selected geometrical parameters are listed in Table 2. Geometrical parameters are defined in Fig. 1.

3.1. Characteristic features of crystal structures

The crystal structures of (1), (2), (3), (4) and (5) observed at room temperature are identical with those reported in the literature (Bürgi *et al.*, 1968; Bürgi & Dunitz, 1970; Meunier-Piret *et al.*, 1972; Filipenko *et al.*, 1976; Ponomarev *et al.*, 1977). The crystal structures of (6) and (7) have not been reported previously.

[1] Supplementary data for this paper are available from the IUCr electronic archives (Reference: BK5007). Services for accessing these data are described at the back of the journal.

3.1.1. Crystal structure of (1). Although no disorder was reported in the previous studies (Bürgi & Dunitz, 1969, 1970), static disorder was detected in this analysis (Fig. 2). Fig. 3 shows difference-Fourier electron density maps of (1) at room temperature and 90 K. Each section contains three C atoms and one N atom (C1, C7, C8 and N1) of the central C—Ph, C═N and N—Ph bonds. At both temperatures two residual peaks (peaks *A* and *B*) near the C7 and N1 atoms were detected. The two peaks correspond to the two atoms of the C═N bond in the second molecule, which is related to the major orientation by a rotation around its shorter axis about 180° (Fig. 2). The structure was refined with a disorder model,

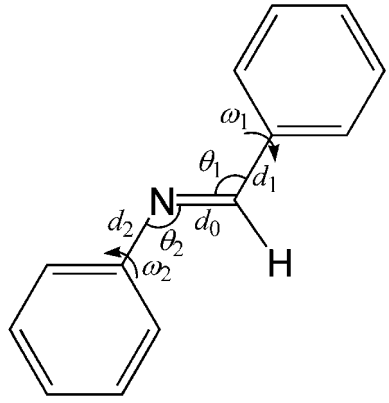

Figure 1
Definition of geometrical parameters for the *N*-benzylideneaniline skeleton.

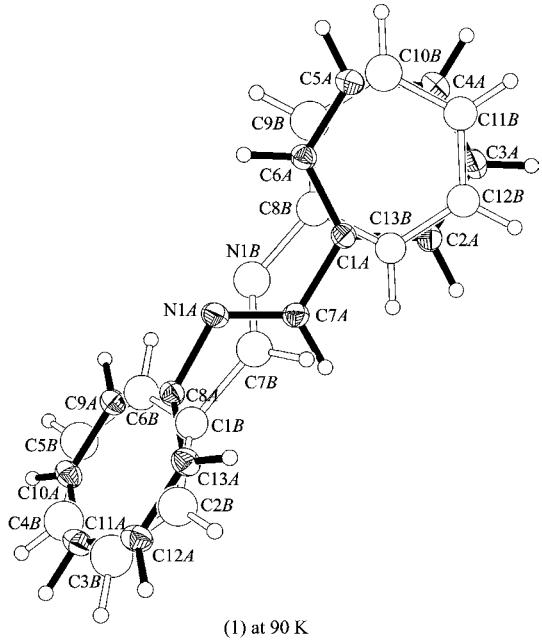

Figure 2
A perspective view of *N*-benzylideneaniline (1) with the atom-numbering scheme. The ellipsoids are drawn at the 50% probability level. H atoms are shown as spheres of a fixed arbitrary size. The major molecule is drawn with filled bonds and shaded ellipsoids. The minor molecule is drawn with open bonds and spheres.

Table 2
Selected geometrical parameters for (1)–(6).

The definitions of the geometrical parameters are given in Fig. 1. The geometrical parameters of (7) are not shown because they were refined under restraints.

			Distance			Bond angle		Torsion angle	
Compound	Origin	T (K)	d_0 (Å)	d_1 (Å)	d_2 (Å)	θ_1 (°)	θ_2 (°)	ω_1 (°)	ω_2 (°)
(1)†	X-ray	300	1.254 (2)	1.466 (2)	1.423 (2)	122.1 (1)	119.4 (1)	9.8 (2)	56.2 (2)
		90	1.276 (1)	1.470 (1)	1.419 (1)	121.1 (1)	118.8 (1)	11.0 (1)	52.6 (1)
	Calc	MP2/6-31G*	1.291	1.465	1.413	121.9	117.4	0.6	46.3
		B3LYP/6-31G*	1.281	1.468	1.406	122.7	120.1	0.8	38.7
(2)	X-ray	300	1.268 (2)	1.473 (2)	1.420 (2)	123.3 (2)	117.1 (2)	12.5 (3)	42.0 (3)
		90	1.281 (2)	1.470 (2)	1.419 (1)	123.3 (1)	116.3 (1)	13.0 (2)	41.4 (2)
	Calc	MP2/6-31G*	1.291	1.464	1.410	121.9	117.4	0.4	48.6
		B3LYP/6-31G*	1.282	1.466	1.401	122.8	120.2	0.7	41.9
(3)	X-ray	300	1.264 (2)	1.467 (2)	1.406 (2)	121.2 (1)	121.6 (1)	8.4 (2)	52.3 (2)
		90	1.281 (1)	1.468 (1)	1.405 (1)	120.3 (1)	121.1 (1)	8.7 (1)	50.4 (1)
	Calc	MP2/6-31G*	1.291	1.462	1.409	122.0	117.5	0.6	49.3
		B3LYP/6-31G*	1.283	1.463	1.398	123.0	120.3	0.9	42.7
(4)	X-ray	300	1.267 (2)	1.467 (2)	1.419 (2)	122.8 (1)	118.3 (1)	15.9 (2)	36.3 (2)
		90	1.281 (1)	1.469 (1)	1.419 (1)	122.4 (1)	117.6 (1)	16.0 (1)	35.6 (1)
	Calc	MP2/6-31G*	1.292	1.465	1.411	121.2	118.0	0.4	39.5
		B3LYP/6-31G*	1.282	1.468	1.402	121.8	121.5	0.8	26.5
(5)‡	X-ray	300, Molecule *A*	1.254 (2)	1.470 (2)	1.422 (2)	123.1 (1)	119.5 (1)	4.0 (2)	28.6 (2)
		90	1.278 (1)	1.468 (1)	1.419 (1)	122.3 (1)	118.5 (1)	3.2 (1)	28.3 (1)
		300, Molecule *B*	1.261 (2)	1.475 (2)	1.419 (2)	121.8 (1)	120.2 (1)	13.1 (2)	40.7 (2)
		90	1.277 (1)	1.473 (1)	1.415 (1)	121.1 (1)	119.5 (1)	15.2 (1)	41.3 (1)
	Calc	MP2/6-31G*	1.291	1.465	1.412	121.2	117.7	0.3	43.1
		B3LYP/6-31G*	1.281	1.469	1.405	121.9	120.8	0.6	33.0
(6)‡	X-ray	300, Molecule *A*	1.261 (2)	1.457 (3)	1.416 (2)	124.0 (2)	120.6 (2)	−6.6 (3)	15.3 (3)
		90	1.279 (1)	1.458 (1)	1.418 (1)	123.0 (1)	119.6 (1)	−7.5 (2)	18.6 (2)
		300, Molecule *B*	1.257 (2)	1.456 (3)	1.419 (2)	124.3 (2)	119.4 (2)	0.3 (3)	34.5 (3)
		90	1.274 (1)	1.460 (1)	1.419 (1)	123.6 (1)	118.1 (1)	0.7 (2)	35.9 (1)
	Calc	MP2/6-31G*	1.291	1.461	1.413	121.9	117.4	0.7	46.3
		B3LYP/6-31G*	1.282	1.463	1.405	122.9	120.1	1.0	38.9

† Geometry of the major orientation in the disordered crystal. ‡ There are two independent molecules in a unit cell.

in which peaks *A* and *B* were assigned as the atoms N1 and C7, respectively. The reverse assignment (*i.e.* peak *A* as C7 and peak *B* as N1) is not valid for the following reasons. Using the correct model (peak *A* as N1 and peak *B* as C7) the torsion angles ω_1 and ω_2 of the minor orientation were found to be 12 (2) and 54 (2)° at 90 K, which are similar to those of the major orientation [11.0 (1) and 52.6 (1)°]. In contrast, the refinement with the incorrect model (peak *A* as C7 and peak *B* as N1) gave different torsion angles [ω_1 = 52 (3) and ω_2 = 13 (3)°]. In the stable conformation of most *N*-benzylideneanlines, the C—Ph bond is not twisted and the N—Ph bond is twisted out of the central C—C=N—C plane. An *ab initio* calculation at the MP2/6-31G* level shows that the torsion angles ω_1 (C—Ph bond) and ω_2 (N—Ph bond) in the most stable conformer of (1) are 0.6 and 46.3°, respectively. Compared with the observed conformer (ω_1 = 10 and ω_2 = 50°), the conformer with reversely twisted geometry (ω_1 = 50 and ω_2 = 10°) was calculated to be 20.3 kJ mol^{-1} higher in energy.

The ratio of the populations of the two orientations was refined to be 0.958 (2):0.042 (2) at room temperature. The ratio remained unchanged as the temperature was lowered [0.946 (1):0.054 (1) at 90 K]. Thus, the disorder is static and no conformational interconversion between the two orientations takes place at and below room temperature.

3.1.2. Crystal structure of (2). Although no disorder was reported in the literature (Bürgi & Dunitz, 1969, 1970), the H atoms of the carboxyl group were found to be disordered (Fig. 4). A similar disorder was reported for the crystal structure of benzoic acid (Bruno & Randaccio, 1980; Feld *et al.*, 1981; Wilson *et al.*, 1996). The populations of the two H atoms refined to 0.52 (4):0.48 (4), 0.55 (3):0.45 (3) at room temperature and 90 K, respectively.

3.1.3. Crystal structure of (3). The methyl H atoms were observed at six positions around the bonded C atom (C14) and refined as two methyl groups with different orientations (Fig. 4). The populations of the two methyl groups refined to 0.60 (2):0.40 (2), 0.58 (6):0.42 (6) at room temperature and 90 K, respectively.

3.1.4. Crystal structure of (4). No disorder was detected at any temperature (Fig. 4).

3.1.5. Crystal structure of (5). There are two crystallographically independent molecules (referred to as molecules *A* and *B* hereafter; Fig. 4). In both molecules the methyl H atoms were found to be disordered and refined as two methyl groups with different orientations. For molecule *A*, the

populations of the two methyl groups refined to 0.57 (3):0.43 (3), 0.83 (2):0.17 (2) at room temperature and 90 K, respectively. For molecule *B* the populations are 0.64 (2):0.36 (2), 0.76 (3):0.24 (3) at room temperature and 90 K, respectively.

3.1.6. Crystal structure of (6). There are two crystallographically independent molecules (Fig. 4). No disorder was observed at any temperature for either molecule.

3.1.7. Crystal structure of (7). In the crystal structure of (7) a static disorder similar to that in crystal (1) was observed (Fig. 5). Fig. 6 shows difference-Fourier electron density maps of (7) at room temperature and 90 K. Each section contains three C atoms and one N atom (C1, C7, C8 and N1) of the central C—Ph, C═N and N—Ph bonds. At both temperatures two residual peaks (peaks *A* and *B*) near the atoms C7 and N1 were detected. The two peaks were assigned to the two atoms of the C═N bond in another misoriented molecule (Fig. 5). The assignment of the two peaks is much easier than that in the crystal of (1) because the two benzene rings of the molecule have different substituents at their *para* positions. In the difference-Fourier maps of (7), three residual peaks (peaks *C*, *D* and *E*) were also detected. The peaks *C*, *D* and *E* can be assigned to the methyl C (C15), methoxy O (O1) and methoxy C atoms (C14) of the minor misoriented molecule, respectively. Peaks *A* and *B* are, therefore, ascribed to the N1 and C7 atoms in the misoriented molecule. With the disorder model the populations of the two orientations refined to 0.932 (3):0.068 (3) at room temperature. The ratio remained unchanged as the temperature was lowered [0.917 (2):0.083 (2) at 90 K]. The disorder is, therefore, static and no conformational interconversion between the two orientations takes place at and below room temperature. In the crystals of (1) and (7) a 180° rotation of the whole molecule around its shorter axis is required for the interconversion between the two orientations. This type of molecular motion seldom occurs in crystals because such a process would suffer from severe steric repulsions by the neighbouring molecules.

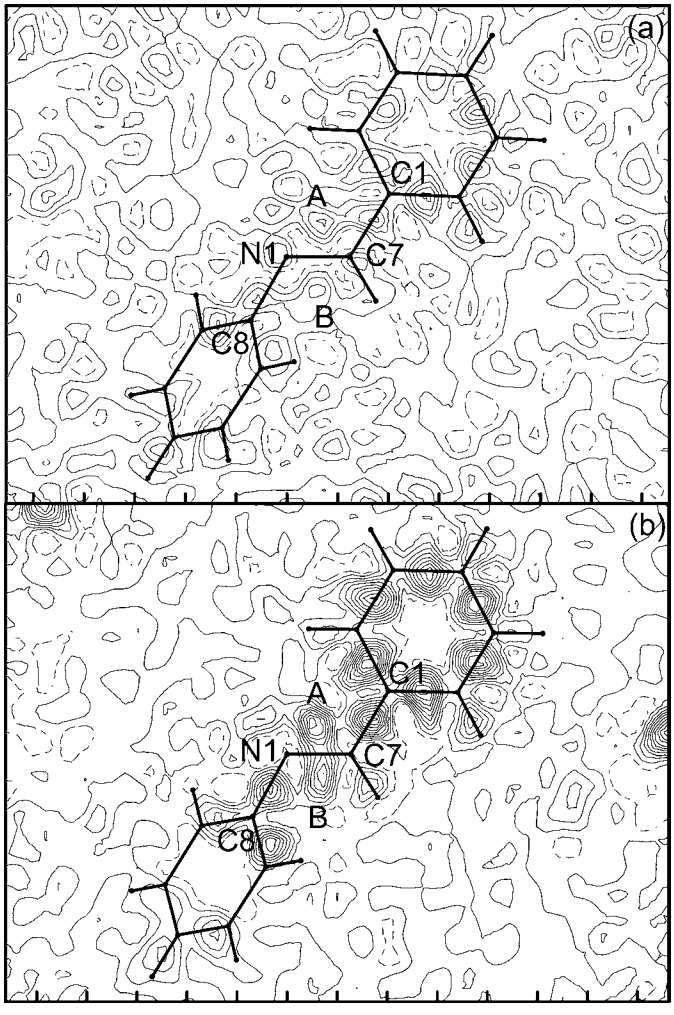

Figure 3
Difference-Fourier maps of *N*-benzylideneaniline (1): (*a*) at room temperature; (*b*) at 90 K. Each section contains three C atoms and one N atom (C1, C7, C8 and N1) of the central C—Ph, C═N and N—Ph bonds. The contour lines are at 0.05 e Å^{-3} intervals. Negative contours are indicated by broken lines.

3.2. Apparent shortening of the C═N bond in the observed structures at room temperature

The observed bond lengths listed in Table 2 clearly show that the C═N bond lengths (d_0) from X-ray diffraction analyses at room temperature are shorter than that calculated (1.29 and 1.28 Å at MP2/6-31G* and B3LYP/6-31G* level, respectively) for all the compounds and that the observed lengths increase at 90 K. The values of the bond angles θ_1 and θ_2 also show a temperature dependence and increase as the temperature is lowered. The extent of the temperature dependence of the bond angles roughly correlates with that of the C═N bond lengths. In spite of the significant temperature dependence of the central C═N bond length, the other bond lengths (*e.g.* d_1, d_2) change little with variation in the temperature and show no anomaly. An apparent shortening of interatomic distances in crystal structures has usually been interpreted in terms of a rotational oscillation of the molecule regarded as a rigid body (the rigid-body model; Cruickshank, 1956; Busing & Levy, 1964). The results for *N*-benzylideneanilines, however, cannot be explained by this model because the temperature dependence of the observed geometry appears only in the central part of the molecules.

3.3. Molecular motion responsible for the apparent shortening of the C═N bond

A similar phenomenon, *i.e.* an apparent shortening and temperature dependence of the central bond length, was observed for the crystals of (*E*)-stilbenes and successfully explained in terms of a torsional vibration of the C—Ph bonds in the crystals (Ogawa *et al.*, 1992, 1995). Crystal structures of azobenzenes and 1,2-diphenylethanes also show an apparent shortening of the central bond length and its temperature dependence due to the torsional vibration of the N—Ph and C—Ph bonds (Harada *et al.*, 1995, 1997; Harada & Ogawa, 2001). The results for *N*-benzylideneanilines can be explained in a similar way.

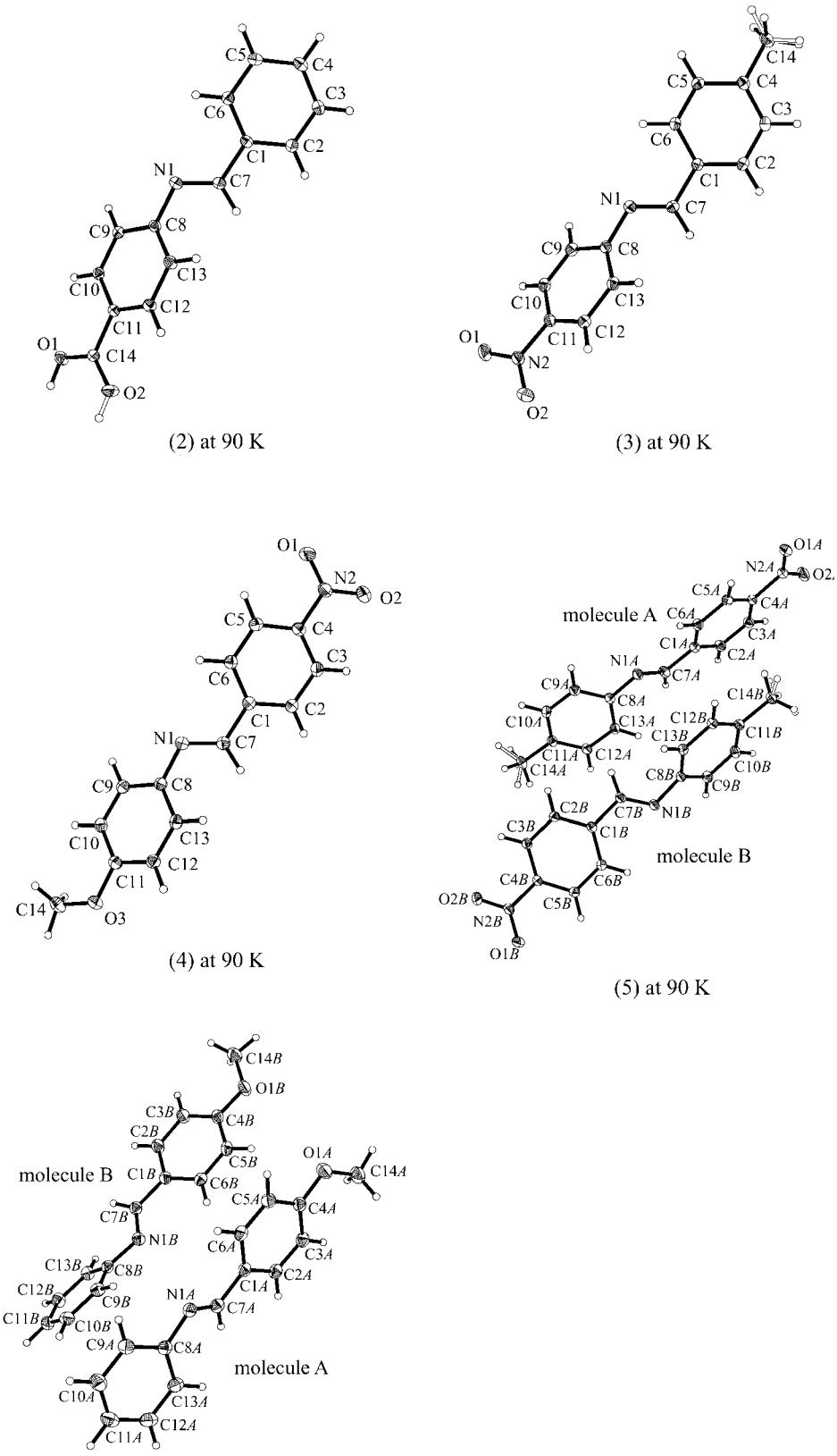

Figure 4
Perspective views of the *N*-benzylideneanilines (2)–(6) with atom-numbering schemes. The ellipsoids are drawn at the 50% probability level. H atoms are shown as spheres with a fixed arbitrary size.

In the crystals of *N*-benzylideneanilines, the torsional vibration of the C—Ph and N—Ph bonds does not change the orientation of the two benzene rings relative to the crystal lattice, but does change that of the C═N moiety (Fig. 7). X-ray diffraction analysis of the crystals gives a structure distorted by thermal motion. The observed structure may be modelled as an average of two conformers, which exist on the torsional potential energy surface but do not correspond to energy minima (Fig. 7). The C═N bond length in the averaged structure appears to be shortened and the two bond angles θ_1 and θ_2 appear to be enlarged. With lowering of the temperature, the amplitude of the vibration and, thus, the separation of the two conformers becomes small and the apparent deformations decrease.

This interpretation is substantiated by the corresponding calculations (Table 3). The molecular structures of five conformers of (1) (*A*–*E*) were obtained by *ab initio* calculations (MP2/6-31G* level). Conformer *C* is the most stable one. The structures of the conformers *A*, *B*, *D* and *E* were optimized with fixed torsion angles. The averaged structure of the two conformers *A* and *E*, whose ω values deviate from those of the most stable conformer (*C*) by $\sim 20^\circ$, corresponds to the structure observed at room temperature. Also, the averaged structure of the two conformers *B* and *D*, whose ω values deviate from those of the most stable conformer by $\sim 10^\circ$, corresponds to the structure observed at 90 K. The observed temperature dependence of the torsion angles of the C—Ph (ω_1) and the N—Ph bonds (ω_2) can be explained if an anharmonicity in the potential energy surface describing the torsional vibration of the C—Ph and N—Ph bonds is assumed.

The C═N bond lengths observed at room temperature differ for different compounds [from 1.254 (2) to 1.268 (2) Å]. The variation of the observed bond lengths can be explained in terms of the variations of the amplitudes of the torsional

vibrations, which depend on the intra- and intermolecular interactions. Invariance of the observed bond length at 90 K [1.274 (1)–1.281 (1) Å] suggests that the amplitude of the torsional vibration is small and that the apparent shortening is negligible at 90 K. The true length of the C═N bond in *N*-benzylideneanilines may therefore be estimated to be 1.28 Å, a value that agrees with those calculated at the B3LYP/6-31G* level, but is 0.01 shorter than those at the MP2/6-31G* level.

Although the C═N bond length at 90 K is largely independent of the substituents, the N—Ph bond length in (3) shows a slight shortening (*ca* 0.01 Å) compared with the other compounds. Compound (3) has a *p*-nitro group in the aniline ring. Accordingly, the shortening may be ascribed to some contribution of a quinoidal structure induced by the electronegative nitro group (Bürgi & Dunitz, 1971).

4. Summary

An apparent shortening of the C═N bonds which depends on temperature was observed in the crystal structures of *N*-benzylideneanilines. They were interpreted in terms of an artifact caused by the torsional vibration of the C—Ph and N—Ph bonds in crystals. At 90 K the C═N bond length was observed to be ∼ 1.28 Å for all the compounds, independent of their substituents. In the crystals of *N*-benzylideneaniline and *N*-(4-methoxybenzylidene)-4-methylaniline, a static disorder was observed.

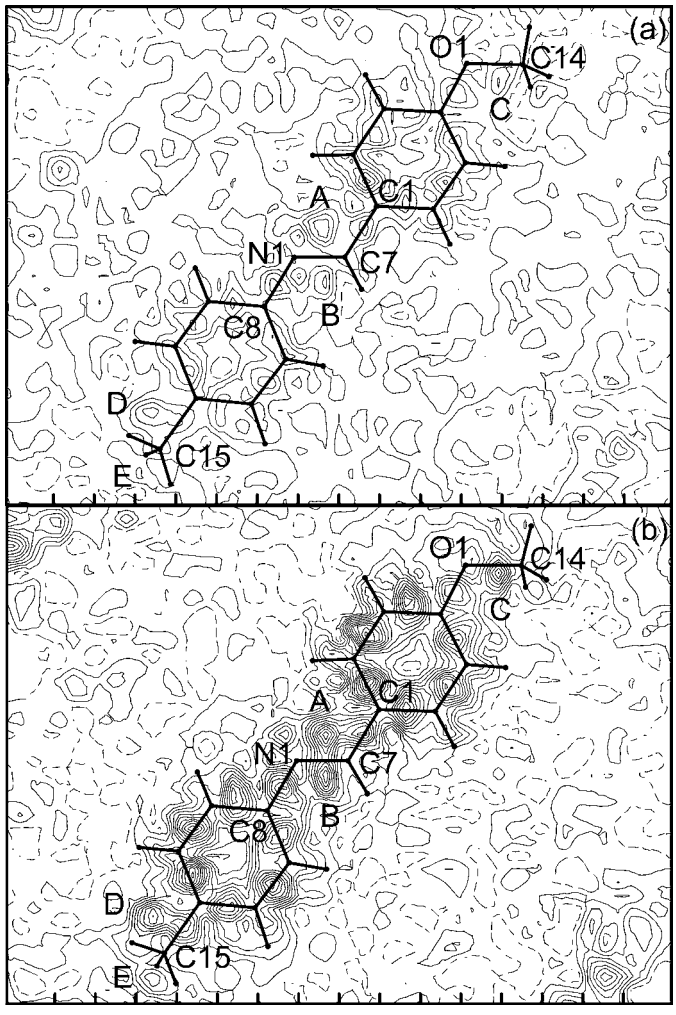

Figure 6
Difference-Fourier maps of *N*-(4-methoxybenzylidene)-4-methylaniline (7): (*a*) at room temperature; (*b*) at 90 K. Each section contains three C atoms and one N atom (C1, C7, C8 and N1) of the central C—Ph, C═N and N—Ph bonds. The contour lines are at 0.05 e Å^{-3} intervals. Negative contours are indicated by broken lines.

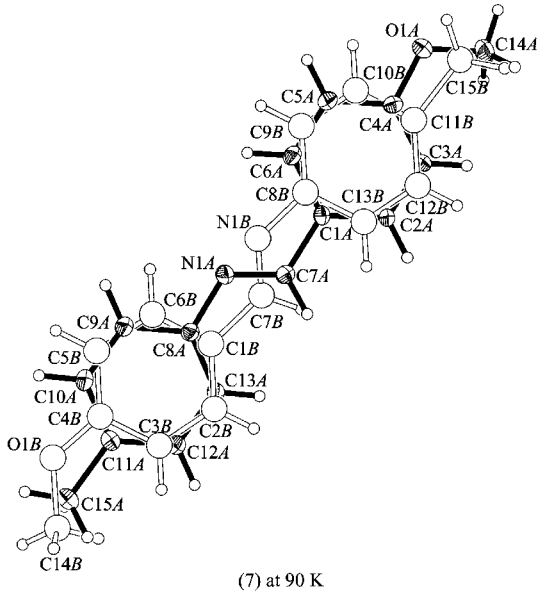

Figure 5
A perspective view of *N*-(4-methoxybenzylidene)-4-methylaniline (7) with the atom-numbering scheme. The ellipsoids are drawn at the 50% probability level. H atoms are shown as spheres of a fixed arbitrary size. The major molecule is drawn with filled bonds and shaded ellipsoids. The minor molecule is drawn with open bonds and spheres.

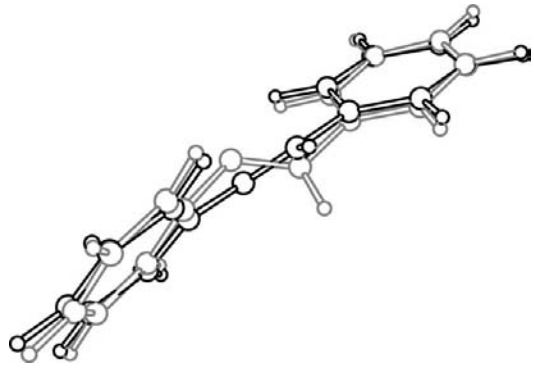

Figure 7
An illustration of the torsional vibration in the crystals of *N*-benzylideneanilines. View of two superimposed conformers in the course of torsional vibration about the C—Ph and N—Ph bonds, during which the two benzene rings do not change their orientation relative to the crystal lattice.

Table 3
Molecular structures of (1) calculated from the torsional vibration model.

Definition of the geometrical parameters is given in Fig. 1. Geometry was optimized at the MP2/6-31G* level.

Structure	d_0 (Å)	d_1 (Å)	d_2 (Å)	θ_1 (°)	θ_2 (°)	ω_1 (°)	ω_2 (°)
A†	1.291	1.465	1.414	121.2	119.3	20.0	25.0
B†	1.291	1.465	1.413	121.6	118.3	10.0	35.0
C	1.291	1.465	1.413	121.9	117.4	0.6	46.3
D†	1.290	1.466	1.414	121.8	116.9	−10.0	55.0
E†	1.290	1.467	1.416	121.6	116.6	−20.0	65.0
(*A* + *E*)/2‡	1.254	1.464	1.411	123.3	120.2	0.1	45.4
(*B* + *D*)/2§	1.282	1.465	1.412	122.2	118.2	0.1	45.1

† Structures *A*, *B*, *D* and *E* were optimized with the torsion angles ω_1 and ω_2 fixed at the given values. ‡ Average of a 1:1 mixture of structures *A* and *E*. § Average of a 1:1 mixture of structures *B* and *D*.

APPENDIX *A*
Refinement of the disordered structures

A1. (1) at room temperature

Only three atoms (N1, C7 and H7) were refined at separate positions in the disorder model. Two atoms of the major conformer (N1*A* and C7*A*) were refined anisotropically and those of the minor conformer (N1*B* and C7*B*) were refined isotropically. The other non-H atoms were refined anisotropically. The H atoms of the C═N bond (H7*A* and H7*B*) were refined according to the riding model. The other H atoms were refined isotropically without any constraint. Populations were determined from the same refinement as above, except that the four disordered atoms (N1*A*, N1*B*, C7*A* and C7*B*) were refined with a common isotropic temperature factor. The populations were held constant during the subsequent anisotropic refinement.

A2. (1) at 90 K

All atoms were refined on separate positions in the disorder model. The benzene rings of the minor conformer were constrained to be regular hexagons with a bond length of 1.39 Å. Non-H atoms of the major conformer (N1*A*—C13*A*) were refined anisotropically and those of the minor conformer (N1*B*—C13*B*) isotropically. H atoms were refined according to the riding model. Populations were determined from the same refinement as above, except that all the non-H atoms were refined with a common isotropic temperature factor. The populations were held constant during the subsequent anisotropic refinement.

A3. (7) at room temperature

Only five atoms (N1, C1, C7, C8 and H7) were refined at separate positions in the disorder model. Four atoms of the major conformer (N1*A*, C1*A*, C7*A* and C8*A*) were refined isotropically and those of the minor conformer (N1*B*, C1*B*, C7*B* and C8*B*) were refined with a single common isotropic temperature factor. The other non-H atoms were refined anisotropically. The H atoms of the C═N bond (H7*A* and H7*B*) were refined according to the riding model. The other H atoms were refined isotropically without any constraint. The length of the C—Ph bond (C1—C7) of the two conformers was restrained to be 1.47 Å with an e.s.d. of 0.01 Å. The length of the N—Ph bond (N1—C8) of the two conformers was restrained to be 1.41 Å with an e.s.d. of 0.01 Å. The lengths of the C═N bonds of the two conformers were restrained to be equal with an e.s.d. of 0.01 Å. In order to restrain the two angles (C1—C7—N1) of the two conformers to be equal, the interatomic distances C1···N1 were restrained to be equal with an e.s.d. of 0.01 Å. In order to restrain the two angles (C7—N1—C8) of the two conformers to be equal, the interatomic distances C7···C8 were restrained to be equal with an e.s.d. of 0.01 Å. Populations were determined from the same refinement as above, except that the eight disordered atoms (N1*A*, N1*B*, C1*A*, C1*B*, C7*A*, C7*B*, C8*A* and C8*B*) were refined with a common isotropic temperature factor. The populations were held constant during the subsequent refinement.

A4. (7) at 90 K

All atoms were refined on separate positions in the disorder model. Non-H atoms of the major conformer (N1*A*—C15*A*) were refined anisotropically. Those of the minor conformer (N1*B*–C15*B*) were refined with a single common isotropic temperature factor. The benzene rings of the minor conformer were constrained to be regular hexagons with a bond length of 1.39 Å. The length of the C—Ph bond (C1—C7) of the two conformers was restrained to be 1.47 Å with an e.s.d. of 0.01 Å. The length of the N—Ph bond (N1—C8) of the two conformers was restrained to be 1.41 Å with an e.s.d. of 0.01 Å. The lengths of the C═N bonds of the two conformers were restrained to be equal with an e.s.d. of 0.01 Å. In order to restrain the two angles (C1—C7—N1) of the two conformers to be equal, the interatomic distances C1···N1 were restrained to be equal with an e.s.d of 0.01 Å. In order to restrain the two angles (C7—N1—C8) of the two conformers to be equal, the interatomic distances C7···C8 were restrained to be equal with an e.s.d. of 0.01 Å. H atoms were refined according to the riding model. Populations were determined from the same refinement as above, except that all the non-H atoms were refined with a common isotropic temperature factor. The populations were held constant during the subsequent anisotropic refinement.

References

Bruker (1998). *SMART* and *SAINT*. Bruker AXS Inc., Madison, Wisconsin, USA.
Bruker (2000). *SHELXTL*, Version 6.10. Bruker AXS Inc., Madison, Wisconsin, USA.
Bruno, G. & Randaccio, L. (1980). *Acta Cryst.* B**36**, 1711–1712.
Bürgi, H. B. & Dunitz, J. D. (1969). *J. Chem. Soc. Chem. Commun.* pp. 472–473.
Bürgi, H. B. & Dunitz, J. D. (1970). *Helv. Chim. Acta*, **53**, 1747–1764.
Bürgi, H. B. & Dunitz, J. D. (1971). *Helv. Chim. Acta*, **54**, 1255–1260.
Bürgi, H. B., Dunitz, J. D. & Züst, C. (1968). *Acta Cryst.* B**24**, 463–464.
Busing, W. R. & Levy, H. A. (1964). *Acta Cryst.* **17**, 142–146.
Cosier, J. & Glazer, A. M. (1986). *J. Appl. Cryst.* **19**, 105–107.
Cruickshank, D. W. J. (1956). *Acta Cryst.* **9**, 757–758.

Ebara, N. (1960). *Bull. Chem. Soc. Jpn*, **33**, 534–539.
Feld, R., Lehmann, M. S., Muir, K. W. & Speakman, J. C. (1981). *Z. Krystallogr.* **157**, 215–231.
Filipenko, O. S., Ponomarev, V. I. & Atovmyan, L. O. (1976). *Dokl. Akad. Nauk. SSSR*, **229**, 1113–1116.
Flack, H. D. (1983). *Acta Cryst.* A**39**, 876–881.
Frisch, M. J. *et al.* (1998). *Gaussian* 98, Revision A.9. Gaussian, Inc., Pittsburgh PA.
Harada, J. & Ogawa, K. (2001). *Struct. Chem.* **12**, 243–250.
Harada, J., Ogawa, K. & Tomoda, S. (1995). *J. Am. Chem. Soc.* **117**, 4476–4478.
Harada, J., Ogawa, K. & Tomoda, S. (1997). *Acta Cryst.* B**53**, 662–672.
Izmailskii, V. A. & Smirnov, E. A. (1956). *Zh. Obshch. Khim.* **26**, 3389–3406.
Jaffe, H. H., Yeh, S.-J. & Gardner, R. W. (1958). *J. Mol. Spectrosc.* **2**, 120–136.
Meunier-Piret, J., Piret, P., Germain, G. & Van Meerssche, M. (1972). *Bull. Soc. Chim. Belg.* **81**, 533–538.
Ogawa, K., Harada, J. & Tomoda, S. (1995). *Acta Cryst.* B**51**, 240–248.
Ogawa, K., Sano, T., Yoshimura, S., Takeuchi, Y. & Toriumi, K. (1992). *J. Am. Chem. Soc.* **114**, 1041–1051.
Ponomarev, V. I., Filipenko, O. S., Atovmyan, L. O., Grazuliene, S., Lempert, S. A. & Shigorin, V. D. (1977). *Kristallografiya*, **22**, 394–396.
Sheldrick, G. M. (1990). *Acta Cryst.* A**46**, 467–473.
Sheldrick, G. M. (1997). *SHELX*97. University of Göttingen, Germany.
Sheldrick, G. M. (2002). *SADABS*, Version 2.03 and 2.05. University of Göttingen, Germany.
Wiegand, C. & Merkel, E. (1942). *Ann.* **550**, 175–181.
Wilson, C. C., Shankland, N. & Florence, A. J. (1996). *J. Chem. Soc. Faraday Trans.* **92**, 5051–5057.